

Available online on 15.09.2019 at <http://ujpr.org>  
**Universal Journal of Pharmaceutical Research**  
 An International Peer Reviewed Journal  
 Open access to Pharmaceutical research  
 This is an open access article distributed under the terms of the Creative Commons  
 Attribution-Non Commercial Share Alike 4.0 License which permits unrestricted non commercial use, provided the  
 original work is properly cited  
**Volume 4, Issue 4, 2019**



## RESEARCH ARTICLE

## EFFECT OF PEGYLATED EDGE ACTIVATOR ON SPAN 60 BASED-NANOVESICLES: COMPARISON BETWEEN MYRJ 52 AND MYRJ 59

Elsaied H. Elsaied\*, Hamdy M Dawaba<sup>1</sup>, El Sherbini A Ibrahim<sup>1</sup>, Mohsen I Afouna<sup>1</sup>

Department of Pharmaceutics and Industrial Pharmacy, Faculty of Pharmacy (Boys), Al-Azhar University, Cairo, Egypt.

### ABSTRACT

In recent years, Span 60 based nanovesicles have been the object of growing scientific attention as an alternative potential drug delivery system to conventional liposomes. Surface modification of nanovesicles can adjust the drug release rate and the affinity for the target site. The aim of present work was firstly to study the effects of different PEGylated edge activator (Myrj 52 and Myrj 59) on Span 60 based nanovesicles. Nanovesicles were prepared using Span 60 alone or in combination with Myrj 52 (polyethylene glycol 2000 monostearate) or Myrj 59 (polyethylene glycol 4400 monostearate) by employing the ethanol injection method. Myrj 52 and Myrj 59 are hydrophilic nonionic surfactants were used to modify the surface of the developed vesicles. Dynamic light scattering was used to determine the size, zeta potential and polydispersity index of the nanovesicles formulation. The vesicles were also characterized for entrapment efficiency and *in vitro* release. In current work, the modified nanovesicles size (ranging from 54.32 to 141.7 nm), zeta potential (ranging from -5.67 to -27.1 mV) and polydispersity index (ranging from 0.248 to 0.531) indicated that the surface modified nanovesicles vesicles are a homogenous and mono-disperse nanovesicles dispersions. The non-modified nanovesicles are showed higher particles size (>2 times) compared to modified nanovesicles. The modified nanovesicles were showed entrapment efficiency ranging from 36.42 to 78.13 %. All the modified nanovesicles showed accepted *in vitro* release of TN from nanovesicles (>70% released after 8 h), followed Higuchi models as drug release mechanism. In conclusion, these surface modified nanovesicles could be used as a potential drug carrier for a variety of drugs.

**Keywords:** Nanovesicles, PEGylated edge activator, Span 60.

**Article Info:** Received 16 July 2019; Revised 12 August; Accepted 9 September, Available online 15 September 2019



### Cite this article-

Elsaied EH, Dawaba HM, Ibrahim ESA, Afouna MI. Effect of pegylated edge activator on Span 60 based-nanovesicles: comparison between Myrj 52 and Myrj 59. Universal Journal of Pharmaceutical Research 2019; 4(4): 1-9.

**DOI:** <https://doi.org/10.22270/ujpr.v4i4.290>

### Address for Correspondence:

**Dr. Elsaied H. Elsaied**, Department of Pharmaceutics and Industrial Pharmacy, Faculty of Pharmacy (Boys), Al-Azhar University, Cairo, Egypt. E-mail: [saidbarakat27@azhar.edu.eg](mailto:saidbarakat27@azhar.edu.eg)

### INTRODUCTION

The self-assembly of non-ionic surfactants into nanovesicles represents an interesting opportunity to achieve vesicular colloidal drug carriers. This resembles liposomes in their architecture and can be used as an effective alternative to liposomal drug carriers<sup>1</sup>. Nanovesicles prepared from non-ionic surfactant are chemically stable, easy stored and of lower cost compared to liposome forming phospholipids<sup>2</sup>. The encapsulation of drug inside the nanovesicles can improve the therapeutic activity of the drug molecules by protecting the drug from biological environment, delayed clearance from the circulation and restricting effects to target cells<sup>3</sup>. The vesicle formation may depend on the HLB value; thus the guidance offered by the HLB number is useful in the evaluation of new classes of compounds for their vesicles forming ability. Span 60 as hydrophobic nonionic surfactant (HLB 4.7) was found to be compatible with vesicle formation<sup>4</sup>.

Modification of the vesicles composition or surface can adjust the drug release rate<sup>5</sup> and the affinity for the target site<sup>6</sup>. A series of research articles were described smart nanovesicles application in drug targeting and delivery<sup>7</sup>. Spanlastic systems recently developed Kakkar and Kauras novel nanovesicles drug carriers based on non-ionic surfactants and explored their potential for the ocular and dermal delivery of ketoconazole. The spanlastic systems consisted of Span 60, as a non-ionic lipophilic surfactant, along with an edge activator (Tween 60 and Tween 80). The edge activators are hydrophilic surfactant molecules that provide flexibility to the lipid bilayer of spanlastic systems by inducing pores and causing destabilization of these membranes<sup>8,9</sup>. Also, long circulation vesicles were recently developed from surface modification of nanovesicles by a hydrophilic carbohydrate or polymer, usually a lipid derivative of polyethylene glycol (PEG), to help evade recognition. The result, called stealth effect, is ascribed to steric stabilization of the vesicles

by the polymer, combined with the additional hydrophilicity that can prevent the adsorption of blood components onto the vesicles surface<sup>10</sup>.

Theophylline (TN) is a widely used methylxanthine drug in the treatment of the patients with moderate to severe reversible bronchospasm. The exploitation of extended release formulation is necessary because of the side effects in clinical practice and associate central nervous system of the fluctuations of serum theophylline level<sup>11</sup>. The serum concentration of theophylline must be maintained within a relatively narrow range to achieve optimal therapeutic benefits while avoiding toxic side effects<sup>12</sup>. Theophylline is rapidly and completely absorbed from liquid preparation, capsules and uncoated tablets<sup>13</sup>.

The aims of the present work to investigate the effect of different PEGylated edge activator (PEA) on Span 60 based nanovesicles taking theophylline as a model drug. Myrj 52 (polyethylene glycol 2000 monostearate) and Myrj 59 (polyethylene glycol 4400 monostearate) were selected as PEA in development of modified nanovesicles. Nanovesicles were characterized by dynamic light scattering in order to determine vesicles size, zeta potential and polydispersity index. We also determined the entrapment efficiency and *in vitro* release properties of the modified nanovesicles. The physicochemical characterization of the modified nanovesicles was compared with those obtained by non-modified nanovesicles.

## MATERIALS AND METHODS

- TN was a kind gift from El-Nile company for pharmaceuticals and chemical industries (Cairo, Egypt)
- Sorbitan monostearate (Span 60), Polyoxyl 40 stearate (Myrj 52) and Polyoxyl 100 stearate (Myrj 59) were purchased from Sigma Chemical Co. (St. Louis, USA).
- Spectra Por<sup>®</sup> semi-permeable membrane (MWCO 12,000–14,000) was obtained from Spectrum Laboratories Inc. (CA, USA).
- All other chemicals and solvents were of analar grade and obtained from El-Nasr Company for pharmaceutical chemicals, Cairo, Egypt.

### Preparation of TN loaded nanovesicles

TN loaded modified nanovesicles were prepared by the ethanol injection method as described by Kakkar and Kaur with some modifications. Briefly, Span 60 was dissolved in ethanol and injected into a preheated aqueous phase in which TN and PEA (Myrj 52 or Myrj 59) was previously dissolved. The organic phase to the aqueous phase ratio was fixed at 1:5. The Span 60: PEA ratios were 9:1, 4:1, 7:3, 3:2 and 1:1, respectively. The nanovesicles were formed spontaneously and turned the resulting hydro alcoholic solution slightly turbid. Continuous stirring of the latter solution on a magnetic stirrer was performed to allow complete evaporation of ethanol<sup>14</sup>. Sonication was performed for 3 min, to promote the development of fine modified nanovesicles. The non-modified nanovesicles were prepared by same method but without adding the PEA.

The composition of the investigated formulae is shown in Table 1.

### Characterization of TN loaded nanovesicles

#### Total drug content

Isopropyl alcohol was chosen as a suitable solvent for disrupting the prepared vesicles. Aqueous nanovesicles dispersion (1 ml) was disrupted by shaking for 15 min in sufficient quantity of isopropyl alcohol and the absorbance of withdrawn aliquot was recorded at 273 nm.

#### Determination of entrapment efficiency of TN in nanovesicles dispersions

Samples (1 ml) of nanovesicles dispersions prepared were frozen for 24 h at -20°C in Eppendorf tubes. The frozen samples were removed from the freezer and let to thaw at room temperature, then centrifuged at 20000 rpm for 60 min at 4°C. Two times washings with phosphate buffer (pH 6.8) were done for complete removal of drug adsorbed on the surface of nanovesicles.

The supernatant was separated each time from nanovesicles pellets and prepared for the assay of free drug. Each result was the mean of three determinations ( $\pm$ SD). The drug content was determined spectrophotometrically against phosphate buffer (pH 6.8) as blank. The % entrapped TN was calculated according to the following equation<sup>15</sup>.

$$\% \text{ EE} = \frac{\text{Total amount of drug} - \text{un entrapped drug}}{\text{Total amount of drug}} \times 100$$

#### Determination of vesicle size, zeta potential and polydispersity index

The hydrodynamic vesicle diameter (z-average) and the polydispersity index (PI) of the systems were evaluated by the dynamic light scattering (DLS) technology via a Zetasizer Nano ZS (Malvern instruments; Worcestershire, UK). The technique analyzes the fluctuations in light scattering due to the Brownian motion of vesicles and consequently estimates z-average. Triplicate measurements were carried out, at 25 $\pm$ 0.5°C, after appropriate dilution with deionized water to obtain a suitable scattering intensity at 90 °C with respect to the incident beam<sup>9</sup>. The better PI values indicate homogenous vesicle size distribution<sup>16</sup>. The zeta potential ( $\zeta$ ) values of the systems were determined according to the electrophoretic light scattering (ELS) technology using a Laser Doppler Anemometer coupled with the same equipment. The technique analyzes the electrophoretic mobility of vesicles under an electric field. Triplicate measurements were carried out, at 25 $\pm$ 0.5°C, after appropriate dilution with deionized water.

#### *In vitro* drug release studies

Based on the calculated EE percentages, accurate amounts of the washed sediments separated from of nanovesicles suspension were redispersed in water. The *in vitro* release of TN from nanovesicles was determined by the dialysis bag method<sup>17</sup> with slight modification. Briefly, 1 ml of nanovesicles dispersion was transferred in dialysis bags with a molecular cut-off 12-14 KDa. The bags were suspended in 100 ml of release medium (phosphate buffer pH 7.4). The whole set-up was placed in a shaking water bath adjusted to a constant speed of 100 rpm at 37 $\pm$ 0.5°C. Samples were

withdrawn at appropriate time intervals from the outer solution to estimate the percentage of drug released. To compensate for sampling, 2 ml of fresh buffer was added to the dissolution media. Two ml of sample was taken from the outer solution at appropriate time intervals, i.e. 1, 2, 3, 4, 5, 6, 7, and 8 h.

The drug released percentages were determined spectrophotometrically at predetermined  $\lambda_{\max}$ . The release studies were conducted in triplicate and the mean drug released percentages ( $\pm$ S.D.) were plotted versus time. Concurrently, the *in vitro* release study of an aqueous TN solution (10 mg/ml) was conducted to investigate the retarding effect of the dialysis tubing.

#### Kinetic analysis

The *in vitro* drug release data were fitted to three different kinetic models which are often used to describe the drug release behavior from nanovesicles, i.e. zero-order, first-order and Higuchi models. Stating the proper mode of release is based on the correlation coefficient ( $r$ ) for the linear regression fit of the parameters involved, where the highest correlation coefficient represents the actual mode of the release<sup>18</sup>.

#### Statistical analysis

The data were reported as mean $\pm$ S.D. ( $n=3$ ) and statistical analysis of the data were carried out using one way ANOVA at a level of significant of  $P < 0.05$ .

#### Ranking the results

The data obtained from the physicochemical evaluation (PZ, PDI, ZP and EE) was ranked and the best formula was selected as nanovesicles model in the development of new carrier for drug delivery. Also, the best formula was subjected to the following investigations.

#### Morphologic examination via transmission electron microscopy (TEM)

The morphologic examination of the systems was carried out to examine the structural attributes such as the lamellarity and the uniformity of size and shape as well as to explore the presence of aggregated vesicles<sup>14</sup>.

A drop of the dispersion was diluted 10-fold using deionized water, and then a drop of the diluted dispersion was applied to a carbon-coated 300 mesh copper grid and left for 1min to allow some of the nanovesicles to adhere to the carbon substrate. The remaining dispersion was removed by absorbing the drop with the corner of a piece of filter paper and the sample was air dried<sup>19</sup>.

#### Fourier transform infrared spectroscopy (FT-IR) studies

The FTIR spectra (range 4000–650  $\text{cm}^{-1}$ ) were performed for TN, Span 60 and PEA using a FT-IR spectrophotometer (spectral resolution of 4  $\text{cm}^{-1}$  and 32 co-added scans) equipped with a MIRacle™ ATR device with a single reflection diamond crystal (1.8 mm spot size). The samples were deposited on top of a diamond crystal and secured with a high-pressure clamp. The average of characteristic peaks of IR transmission spectra were recorded from triplicate samples<sup>9</sup>.

#### Differential scanning calorimetry (DSC)

For thermal analysis, samples were scanned using DSC and the thermograms so generated were evaluated for any significant shift or disappearance/appearance of

new peaks. Assessment the degree of crystallinity and the presence of possible interactions between TN, Span 60 and PEA were explored by using DSC techniques. The calorimeter was calibrated for temperature and heat flow accuracy using the melting of pure indium (m.p.156.6°C and  $\Delta H$  of 25.45 J  $\text{gm}^{-1}$ ). The temperature range was from 0 to 300°C with a heating rate of 10°C/min. The gas used was nitrogen with a purging rate of 50 ml/min<sup>14</sup>.

#### Stability studies

Stability studies were carried out to investigate the leaching of drug from nanovesicles during storage. The ability of vesicles to retain the drug was assessed by keeping the nanovesicles suspension in sealed glass ampoules (15 ml capacity) at 25°C, and 4°C for 3 months. Samples were withdrawn periodically and analyzed for entrapment efficiency and drug content.

## RESULTS AND DISCUSSION

### Formation of TN-loaded nanovesicles

Span 60 were selected in nanovesicles preparation based on preliminary study which performed on nanovesicles prepared from different Spans (Span 20, Span 40, Span 60 and Span 80) at the same concentration, to investigate the influence of surfactant structure on TN entrapment efficiency. Nanovesicles prepared from Span 60 exhibit high entrapment efficiency than other Spans. Span 60 has higher phase transition temperature which plays a vital role in the degree of entrapment efficiency. Span 80 has the oleate side chain which has one unsaturated double bond making the oleate chain bend and the adjacent molecular cannot be tight when they form the nanovesicles membrane<sup>20</sup>. In addition, Span 80 has the lowest transition temperature<sup>21</sup> among all tested span surfactants.

Span 60 based nanovesicles were successfully prepared, in the presence of Myrj52, Myrj 59 or alone, by the ethanol injection method. The method of preparation of nanovesicles is based on the simple idea that the mixture of surfactant: alcohol: aqueous phase can be used to form nanovesicles dispersions. Many synthetic amphiphiles such as nonionic surfactants, quaternary ammonium salts with one, two or three chains and long chain fatty acids were able to form bilayers under favorable conditions<sup>15</sup>. A bilayer is normally constituted of a long chain amphiphiles, with a hydrophilic head and a hydrophobic tail<sup>22</sup>. The transfer of hydrocarbon chains into aqueous medium would accompany a free energy loss originating mainly from entropy which drives the organic layer into ordered bilayers<sup>23</sup>.

The lipophilic nature of the saturated alkyl chains in Span 60 would permit the formation of mono and/or multi-lamellar matrix vesicles<sup>24</sup>. In a parallel line, the surface active properties of this surfactant would augment the action of the hydrophilic surfactants allowing for a reduction in the interfacial tension and subsequent development of fine nanovesicles dispersions<sup>9</sup>. Myrj 52 and Myrj 59 are hydrophilic nonionic surfactants with HLB 16.9 and 18.8; respectively<sup>25</sup>.The incorporation of PEA (Myrj 52 or Myrj 59) can destabilize the vesicular membranes,

increase their deformability and create systems having different degrees of disruption in packing characteristics<sup>26</sup>. Furthermore, these hydrophilic surfactants would potentiate the elastic nature of the vesicles allowing them to temporarily increase the pore size of the biological membranes such that slightly bigger vesicles can squeeze in and promote better drug penetration<sup>27</sup>.

Ethanol has positive impacts on the properties of these nanovesicles via improving the drug partitioning and entrapping within the vesicles<sup>28</sup>, via decreasing the size of the vesicles by the reduction of the thickness of their membranes due to the membrane condensing ability of ethanol or the formation of a phase with interpenetrating hydrocarbon chains and finally via modifying the net charge of the system toward a negative zeta potential resulting in some degree of steric stabilization<sup>29</sup>.

### Characterization of TN loaded nanovesicles

#### Drug content

The amount of TN added into the nanovesicles dispersions was 5 mg/ml and the drug content of the developed formulations was not found to be significantly different ( $p < 0.05$ ) from the added amount (Table 2).

#### Entrapment efficiency

In freezing, drug and vesicles are concentrated; particles are closely packed in contact with each other resulting in fusion of nanovesicles<sup>21</sup>. The EE percentages of TN-loaded non-modified nanovesicles dispersion (Nvs11) was 56.60% while the EE percentages of TN-loaded surface modified nanovesicles dispersion (Nvs1-Nvs10) varied markedly from 76.13% (Nvs1) to 36.42% (Nvs10), as shown in Table (2). The ANOVA results confirmed that the PEA type and concentration had significant impacts ( $P < 0.05$ ) on the EE% of the developed formulae. Myrj 52 decorated vesicles showed significantly higher EE % than the corresponding Myrj 59 decorated ones. The significantly higher drug EE percentages of the PEA low concentration (10%) dispersions ( $p < 0.001$ ) could be attributed to the ability of the polar head groups of PEA to solubilize higher drug amounts via hydrogen bonding with the carboxyl groups. In fact, increases the concentrations of PEA above 10% lower drug EE percentages were obtained. According to<sup>30</sup>, when the PEA concentration reaches a certain threshold, vesicles size decrease (SUV) and consequently decrease the EE%.

Results listed in Table 2 showed that nanovesicles developed from Myrj52 mainly have higher entrapment efficiency than other formulations containing Myrj 59 this could be due to the PEA chemical structure.

Nanovesicles prepared from Myrj 52 were exhibit high entrapment efficiency this could be explained on the basis that the ability of Myrj 52 to form hydrogen bond with Span 60 and the increase in Myrj 52 concentration and/or hydrophilicity would enhance the bending of these chains to a degree that can affect the tightness of the developing vesicular membranes<sup>9</sup>. These effects can increase the tendency of TN escape and the membrane permeability.

### Vesicle size and polydispersity index (PDI)

This study shows that the particle size of non-modified nanovesicles (Nvs11) was 287.8 nm while the particle size of non-modified nanovesicles formulations lies between 54.32-141.7 nm which is a convenient nano-range. Table 3 showed significant decrease of particle size upon addition of PEA (Myrj 52 and Myrj 59) in comparison with Nvs11. Also, significant decrease of particle size upon increasing concentration of PEA (Myrj 52 and Myrj 59) above 30% and decreasing the concentration of Span 60 in comparison with 10-20% of PEA. This indicates that the particle size of the prepared nanovesicles was influenced by the type and concentration of the PEA. The increase of PEA concentration reduces the size of nanovesicles<sup>9</sup>. This is attributed to the reduction in the surface tension between the aqueous phase and the organic phase and the diminution of the latter one decreases the particles size<sup>14</sup>. In formulations containing Myrj 52, the particle size was found to be higher than formulation containing Myrj 59 at same concentration. This might be due to the higher emulsification power of Myrj 59 than Myrj 52. The PEA are hydrophilic nonionic surfactant molecules that provide flexibility to the lipid bilayer membranes of nanovesicles. These surfactant molecules destabilize the lipid bilayer and, in turn, increase the deformability of the vesicles. The surfactant present in these vesicles causes them to induce pores in lipid structures, such as membranes, and also provokes a solubilization in the higher concentration range<sup>27</sup>.

The ANOVA results showed that higher edge activator concentration above 30% had significant effects ( $P < 0.05$ ) on the mean vesicle size of the developed spanlastic vesicles.

Generally, inverse correlations were observed between the PEA concentration and the mean vesicle size. This might be attributed to the increasing emulsification power encountered with the use of higher concentrations of the PEA. It could be inferred that the lower PEA concentrations might be unable to cover the entire vesicle surface. Thereby, some vesicles would aggregate till the surface area is decreased to a point that the available amount of the PEA was able to coat the entire surface of the agglomerate and thus forming a stable dispersion. In a parallel line, the increase in the vesicle size with increasing Span 60 concentrations was correlated to the insertion of more alkyl chains of Span 60 into the hydrophobic domain of the vesicles and the subsequent reduction in the interaction between the polar heads of the PEA molecules<sup>31</sup>.

The obtained PDI values of non-modified nanovesicles was 0.634 and the PDI values of modified nanovesicles were lies between 0.248 – 0.531 as shown in Table 3, which shows that the particle size populations of the Nvs1 and Nvs2 are very homogeneous. These good results of particle size and PDI of TN loaded surface modified nanovesicles.

#### Zeta potential

The surface charge of the vesicles controls their stability in nanovesicles formulations through strong electrostatic repulsions between the particles<sup>32</sup>. Table 3 shows that the Nvs1, Nvs2 and Nvs11 in this study

display a sufficiently high negative zeta potential that ensures that the nanoparticles will disperse very well in the aqueous media and that the nano suspension will have a very good stability and tolerance against aggregation<sup>33</sup>.

It was clear from Table 3 that the zeta potential of non-modified nanovesicles is -30.41 mV and all the modified nanovesicles were acquired negative value of zeta potential lie between -5.67 mV to -27.1 mV. Generally the negative zeta potential values are expected due to the membrane condensing ability of ethanol or the formation of a phase with interpenetrating hydrocarbon chains and finally via modifying the net charge of the system toward a negative zeta potential resulting in some degree of steric stabilization<sup>29</sup>.

All the developed nanovesicles were negatively charged which is in agreement with similar results obtained by Tayel and colleagues, which predict a good stability of the prepared nanovesicles. The results showed that the highest zeta potential value (-30.41 mV) was obtained in case of the formulation Nvs11 while the lowest zeta potential value (-5.67 mV) was obtained in case of the formulation Nvs4. The difference in zeta potential values could be explained by the fact that the stability is dependent on the combination of the Span 60 with PEA. This is attributed to differences in the PEA concentration which leading to differences in surface coverage.

#### **In vitro release profile of theophylline**

Figure 1 and Figure 2 showed that the release profiles of TN from modified and non-modified nanovesicles of different PEA contents is an apparently biphasic release process. Rapid drug leakage was observed during the initial phase ranged from 25 – 57% of the entrapped drug was released from various formulations in the first 30 min of nanovesicles suspended in 100 ml of phosphate buffer pH 7.4. However, during the following 8 h a slow release occurred in which most of TN was released from different nanovesicles preparations (about 73-99%). This could be explained on the basis that the drug is mainly incorporated between the fatty acid chains in the lipid bilayers of nanovesicles. This leads to rapid ionization and release upon dispersing nanovesicles in increased buffer volumes until reaching equilibrium. Also, it has been reported that, a highly ordered lipid particles cannot accommodate large amounts of drug and is the reason for drug expulsion<sup>34</sup>.

Different nanovesicles dispersions were tested for the drug release behavior in order to evaluate the effect of PEA/Span 60 ratio on TN release. The observed differences in release characteristics could be attributed to the EPA type and concentration in the formulation. Figure 1 and Figure 2 showed that the non-modified nanovesicles formulations displayed 50.67% released after 8 h and the modified nanovesicles containing 10% EPA (Nvs1 and Nvs6) displayed the lowest extent of drug release after 8hrs (73.22% and 73.21%) in phosphate buffer pH 7.4. In addition to, Nvs10 showed higher release rates after 8hrs (about 99.5%) at phosphate buffer pH7.4 compared to other formulations. The increase in release rates of TN from

nanovesicles formulation upon increase PEA content was statistically significant ( $P < 0.05$ ).

The correlation between the PEA concentration and the drug released percentages could be explained with respect to the vesicle diameters, the amount of the dissolved drug in the lipophilic part increase as the radius of the vesicles increase. Also, at higher EPA, the smaller vesicles would reduce the drug diffusional distance and consequently promote higher drug dissolution rates<sup>35</sup>. Figure 1 and Figure 2 showed the difference in the release rates between the nanovesicles containing Myrj 52 and nanovesicles containing Myrj 59. Significantly ( $P < 0.05$ ) higher drug released percentages were achieved with nanovesicles containing Myrj 59 at concentration above 30% (more than 93% released). Statistical analysis showed non-significant differences in the release percentages of TN from Nvs1 and Nvs6 in different pH systems after 8 h ( $P = 0.601$ ). The result is in accordance with Tayel and colleagues who reported that increasing edge activator concentration can disrupt the regular linear structure of the vesicular membrane and increase the drug release<sup>34</sup>.

#### **Kinetic analysis of the release data of TN- loaded nanovesicles**

The obtained release data were tested according to zero, first order kinetic and diffusion controlled model. The pattern of TN release from nanovesicles formulations was in favor of Higuchi models.

#### **Ranking the results**

From the total rank order as shown in Table 4, it can be concluded that Nvs1 is the best one according to the data obtained from the physicochemical evaluation (PZ, PDI, ZP and EE). Also, Nvs1 showed accepted total drug content and *in vitro* release of TN from nanovesicles, followed Higuchi model drug release mechanism. So, Nvs1 was selected as drug carrier system and subject to further characterization.

#### **Morphological Characterization**

The morphological appearance of Nvs1 was visualized using transmission electron microscope (TEM) and the obtained photographs were illustrated in Figure 3. The examined nanovesicles appeared as small unilamellar (SUV), spherical nanovesicles under the TEM. The morphologic examination of the dispersions confirmed the development of nano spherical vesicles having narrow size distributions; in accordance with the results of the particle size measurements. The smaller vesicles were almost unilamellar with larger internal aqueous cores.

#### **FT-IR studies**

FT-IR spectroscopic studies were employed to explore the possible intermolecular interactions between TN, Span 60 and Myrj 52. The FT-IR spectra of TN, Span 60, Myrj 52 and physical mixture are displayed in Figure 4. The characteristic peaks of TN were compared with the peaks obtained for their formulation. It was observed that similar characteristic peaks appear with minor differences, the peaks appearing in region 2824–2712  $\text{cm}^{-1}$  are attributed to N=CH3 bond. The C-N stretching vibrations are seen at 1049  $\text{cm}^{-1}$ , while the one that appeared at 1243  $\text{cm}^{-1}$  is assigned to aromatic C=O stretching vibrations. A slight shift of bands position from 1717  $\text{cm}^{-1}$  to 1712

cm<sup>-1</sup> and from 1667 cm<sup>-1</sup> from 1663 cm<sup>-1</sup> attributed to CO-N(R)-CO theophylline characteristic group. The bands at 3430–3450 cm<sup>-1</sup> assigned to OH groups and also band at 2882 cm<sup>-1</sup> assigned to CH<sub>2</sub> symmetric stretching because of the possible interactions between components by hydrogen bonding. The bands at 2862 cm<sup>-1</sup> and 2923 cm<sup>-1</sup> could be attributed to C-H stretching vibrations of methyl and/or methylene groups of Span 60 and Myrj 52, respectively. The FT-IR spectrum of the physical mixture revealed that the characteristic bands of TN did not disappear or exhibit major shifts. Furthermore, no new bands were formed. These findings point out the lack of considerable intermolecular interactions between TN, Span60 and Myrj 52 as shown in Figure 4.

#### Differential scanning calorimetry (DSC)

Figure 5 depicts various DSC thermograms obtained during the study. Pure TN showed a sharp endothermic peak at 273°C. Thermogram of Span 60 exhibits an endothermic peak with onset at 44.62°C and maximum occurrence at 52.24°C. Myrj 52 showed an endothermic peak at 52.6°C. The DSC thermograms of developed nanovesicles showed new endothermic peak at 106.4°C, indicating an increase in the phase transition temperature of nanovesicles upon loading with TN. These findings could point out the possible dispersion of TN throughout the nanovesicular carrier in an amorphous state<sup>9</sup>. The TN peak was disappeared upon incorporation of TN into nanovesicles proving complete entrapping of drug into the vesicles.

#### Stability studies

The results of stability studies are compiled in Figure 6. Stability of vesicles is referred to in terms of % loss in drug content and % of drug entrapped in vesicles over a period of 1, 2 and 3 months of storage. Extent of drug leanness upon storage in refrigerator was significantly low; while at room temperature there was an appreciable drug loss and decreased in entrapment efficiency (10% and 30%). Hence the system needs to be refrigerated for use as is the case with all other vesicular systems. Developed modified nanovesicles were sufficiently stable under refrigerated condition and fulfill ICH guidelines showing 2.09% loss in drug content and 5% decreased in entrapment efficiency at 3 months. However, the formulations are not recommended to be stored at room temperature.

#### CONCLUSION

From the above mentioned results, we can conclude that; Surface modified nanovesicles were successfully prepared by the ethanol injection method. The particle size obtained for the investigated modified nanovesicles formulations were in the submicron range (from 54.3-141.7nm) with PDI less than 0.5 and negative charge. Modified nanovesicles showed high drug encapsulation efficiencies and higher release rate. From the statistical analysis to the obtained results of nanovesicles formulation, increased amount of PEA caused decrease in the particle size, zeta potential and the % entrapment efficiency for the developed nanovesicles formulation. The TEM images of the modified nanovesicles, showing the formation of uniform, regular round spherical in shape and smooth

surface nanovesicles with no evidence of aggregation. Finally, the surface modified nanovesicles are a promising drug carrier system.

#### CONFLICT OF INTEREST

No conflict of interest was associated with this work.

#### REFERENCES

- Dan N. Core-shell drug carriers: liposomes, polymersomes, and niosomes', in nanostructures for drug delivery (Elsevier, 2017), 63-105.
- Marianecci C, Marzio LD, Rinaldi F, Celia C, Paolino D, Alhaique F, Esposito S, Carafa M. Niosomes from 80s to Present: The State of the Art', *Advances in colloid and interface science* 2014; 205:187-206.
- Ingallina C, Rinaldi F, Bogni A, Ponti J, Passeri D, Reggente M, Rossi M, Kinsner-Ovaskainen A, Mehn D, Rossi F. Niosomal approach to brain delivery: development, characterization and *in vitro* toxicological studies. *Int J pharmaceutics* 2016; 511:969-82.
- Lohumi A. A novel drug delivery system: niosomes review. *J Drug Deliv Therap* 2012; 2.
- Rania S Abdel-Rashid, Doaa A Helal, Mahmoud M Omar, and Amani M El Sisi, 'Nanogel Loaded with Surfactant Based Nanovesicles for Enhanced Ocular Delivery of Acetazolamide', *Int J nanomed* 2019; 14:2973.
- Cui W, Li J, Decher G. Self-assembled smart nanocarriers for targeted drug delivery. *Advanced Mat* 2016; 28:1302-11.
- Marianecci C, Carafa M. Smart nanovesicles for drug targeting and delivery. *Multidisciplinary Digital Publishing Institute*, 2019.
- Abbas H, Kamel R. Potential role of resveratrol-loaded elastic sorbitan monostearate nanovesicles for the prevention of UV-induced skin damage. *J Liposome Res* 2019; 1-9.
- Tayel SA, El-Nabarawi MA, Tadros MI, Abd-Elsalam WH. Duodenum-triggered delivery of pravastatin sodium via enteric surface-coated nanovesicular spanlastic dispersions: development, characterization and pharmacokinetic assessments. *Int J Pharm* 2015; 483:77-88.
- Moghimi SM, Szebeni J. Stealth liposomes and long circulating nanoparticles: critical issues in pharmacokinetics, opsonization and protein-binding properties. *Progress in lipid Res*; 2003; 42:463-78.
- Mastholimath VS, Dandagi PM, Jain SS, Gadad AP, Kulkarni AR. Time and Ph dependent colon specific, pulsatile delivery of theophylline for nocturnal asthma. *Int J Pharm* 2007; 328: 49-56.
- Marsha A Raebel *et al.* Monitoring of drugs with a narrow therapeutic range in ambulatory care. *American J Managed Care* 2006; 12:268-75.
- Weinberger M, Hendeles L. Theophylline in Asthma. *New England J Medicine*, 1996; 334:1380-88.
- Kakkar S, Kaur IP. Spanlastics -a novel nanovesicular carrier system for ocular delivery. *Int J pharm* 2011; 413:202-10.
- Alsarra IA, Bosela AA, Ahmed SM, Mahrous GM. Proniosomes as a drug carrier for transdermal delivery of ketorolac. *European J Pharm Biopharm* 2005; 59:485-90.
- Balakrishnan P *et al.* Formulation and *in vitro* assessment of minoxidil niosomes for enhanced skin delivery. *Int J pharmaceutics* 2009; 377: 1-8.
- Bayindir ZS, Yuksel N. Characterization of niosomes prepared with various nonionic surfactants for paclitaxel oral delivery. *J Pharm Sci* 2010; 99:2049-60.
- Guinedi AS, Mortada ND, Mansour S, Hathout RM. Preparation and evaluation of reverse-phase evaporation and multilamellar niosomes as ophthalmic carriers of acetazolamide. *Int J Pharm* 2005; 306:71-82.
- Ammar HO, Ghorab M, El-Nahhas SA, Higazy IM. Proniosomes as a carrier system for transdermal delivery of tenoxicam. *Int J Pharmaceutics* 2011; 405:142-52.

20. Arora R. Advances in niosome as a drug carrier: a review. *Asian J Pharm* 2007; 1(1):29-39.
21. Mokhtar M, Sammour OA, Hammad MA, Megrab NA. Effect of some formulation parameters on flurbiprofen encapsulation and release rates of niosomes prepared from proniosomes. *Int J Pharmaceutics* 2008; 361:104-11.
22. Zulauf M. Detergent phenomena in membrane protein crystallization', in *Crystallization of Membrane Proteins* (CRC Press) 2018; 53-72.
23. Thomas PJ, Lavanya A, Sabareesh V, Kulkarni GU. Self-assembling bilayers of *palladium thiolates* in organic media. *J Chem Sci* 2001; 113:611-19.
24. Ching-Yun H et al. Intravenous anti-mrsa phosphatiosomes mediate enhanced affinity to pulmonary surfactants for effective treatment of infectious pneumonia. *Nanomedicine: nanotechnology, biology and medicine* 2018; 14:215-25.
25. Schmidts T, Dobler D, Nissing C, Runkel F. Influence of hydrophilic surfactants on the properties of multiple W/O/W emulsions. *J Colloid Int Sci* 2009; 338:184-92.
26. Trotta M, Peira E, Carlotti ME, Gallarate M. Deformable liposomes for dermal administration of methotrexate. *Int J pharmaceutics* 2004; 270:119-25.
27. Kaur IP et al. Development and evaluation of novel surfactant-based elastic vesicular system for ocular delivery of fluconazole. *J Ocular Pharm Therap* 2012; 28:484-96.
28. Ahad A, Aqil M, Kohli K, Sultana Y, Mujeeb M. Enhanced transdermal delivery of an anti-hypertensive agent via nanoethosomes: statistical optimization, characterization and pharmacokinetic assessment. *Int J Pharm* 2013; 443:26-38.
29. Lasic DD. Novel applications of liposomes', trends in biotechnology 1998; 16:307-21.
30. Bergh BAI, Wertz PW, Junginger HE, Bouwstra JA. Elasticity of vesicles assessed by electron spin resonance, electron microscopy and extrusion measurements. *Int J Pharmaceutics* 2001; 217:13-24.
31. Junyaprasert VB, Singhsa P, Suksiriworapong J, Chantasant D. Physicochemical properties and skin permeation of span 60/Tween 60 niosomes of ellagic acid. *Int J Pharm* 2012; 423:303-11.
32. Honary S, Zahir F. Effect of Zeta Potential on the properties of nano-drug delivery systems-a review (Part 2)'. *Tropical J Pharm Res* 2013; 12:265-73.
33. Uskoković V, Odsinada R, Djordjevic S, Habelitz S. Dynamic light scattering and zeta potential of colloidal mixtures of amelogenin and hydroxyapatite in calcium and phosphate rich ionic milieu. *Archives Oral Biol* 2011; 56:521-32.
34. Wissing SA, Kayser O, Müller RH. Solid lipid nanoparticles for parenteral drug delivery. *Adv Drug Deliv Rev* 2004; 56:1257-72.
35. Wacker M. Nanocarriers for intravenous injection—the long hard road to the market. *Int J Pharmaceutics* 2013; 457:50-62.

**Table 1: The composition (mg/ml) of TN loaded nanovesicles.**

Formula	Span 60 (mg)	Myrj 52 (mg)	Myrj 59 (mg)	TN (mg)
Nvs1	45	5	-	5
Nvs2	40	10	-	5
Nvs3	35	15	-	5
Nvs4	30	20	-	5
Nvs5	25	25	-	5
Nvs6	45	-	5	5
Nvs7	40	-	10	5
Nvs8	35	-	15	5
Nvs9	30	-	20	5
Nvs10	25	-	25	5
Nvs11	50	0	0	5

**Table 2: Total drug content and % entrapment efficiency of nanovesicles (each result is the mean ± SD, n= 3)**

Formula	Total drug content	Entrapment Efficiency %
Nvs1	4.98±0.37	76.13±0.54
Nvs2	4.91±0.55	62.40±1.02
Nvs3	4.90±0.75	50.66±0.83
Nvs4	4.88±1.09	44.34±0.99
Nvs5	4.85±1.02	40.16±0.49
Nvs6	4.95±0.29	67.20±0.09
Nvs7	4.90±0.10	57.65±1.11
Nvs8	4.87±0.81	42.01±0.68
Nvs9	4.86±1.06	37.56±0.96
Nvs10	4.84±0.83	36.42±0.99
Nvs11	4.81±1.23	56.60±1.06

Table 3: The mean vesicles size, polydispersity index and zeta potential of nanovesicles formulation.

Formula	Mean vesicles size (nm)	PDI	Mean Zeta potential (mV)
Nvs1	139.3	0.325	-27.1
Nvs2	141.7	0.248	-26.7
Nvs3	103.8	0.362	-11.1
Nvs4	76.63	0.400	-5.67
Nvs5	73.47	0.531	-11.3
Nvs6	131.7	0.397	-6.44
Nvs7	97.66	0.429	-6.36
Nvs8	90.42	0.488	-7.76
Nvs9	75.02	0.436	-6.95
Nvs10	54.32	0.399	-6.24
Nvs11	287.8	0.634	-30.41

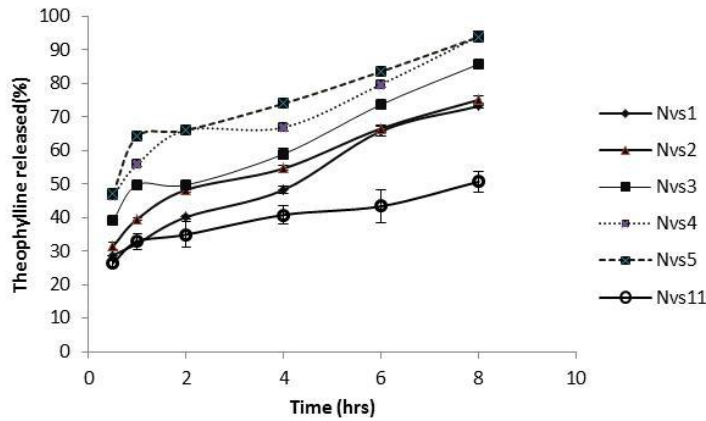


Figure 1: Effects of Myrj 52 concentration on TN release from nanovesicles at pH 7.4.

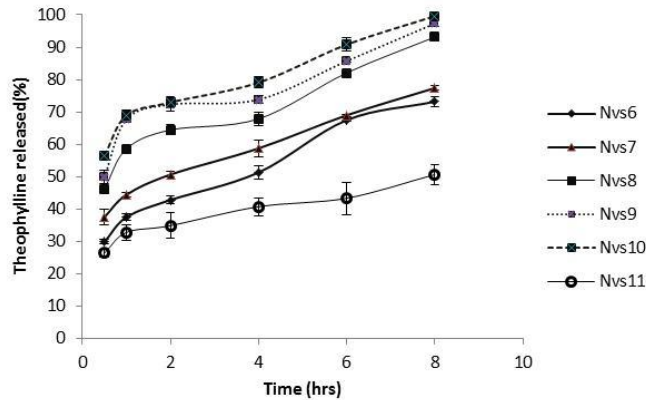


Figure 2: Effects of Myrj59 concentration on TN release from nanovesicles at pH 7.4.

Table 4: Rank order for the physicochemical evaluation of TN loaded nanovesicles.

Formula	EE % rank Order	particle size rank order	PDI rank Order	Zeta potential rank order	Total rank Order
Nvs1	1	9	2	2	14
Nvs2	3	10	1	3	17
Nvs3	6	7	3	5	21
Nvs4	7	4	6	11	28
Nvs5	9	2	10	4	25
Nvs6	2	8	4	8	22
Nvs7	4	6	7	9	26
Nvs8	8	5	9	6	28
Nvs9	10	3	8	7	28
Nvs10	11	1	5	10	27
Nvs11	5	11	11	1	28

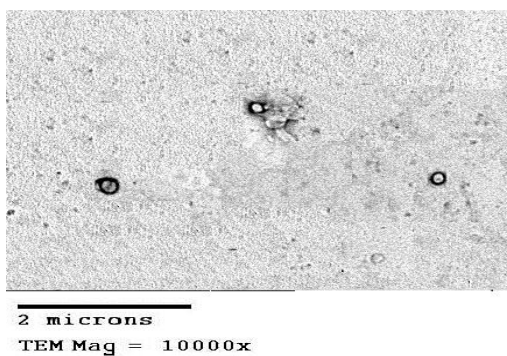


Figure 3: TEM micrographs of vesicles at 10000x magnification of Nvs1.

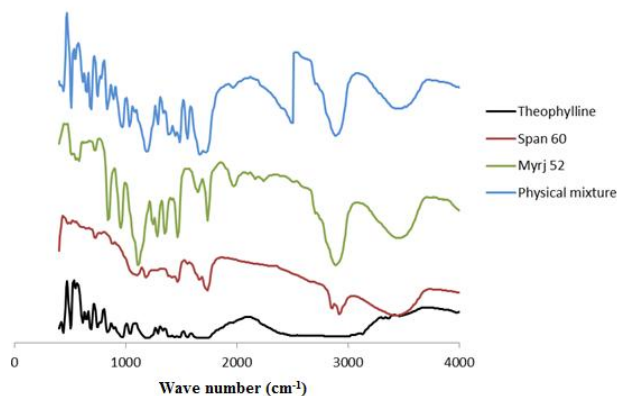


Figure 4: FT-IR spectra of TN, Span 60, Myrj 52 and physical mixture

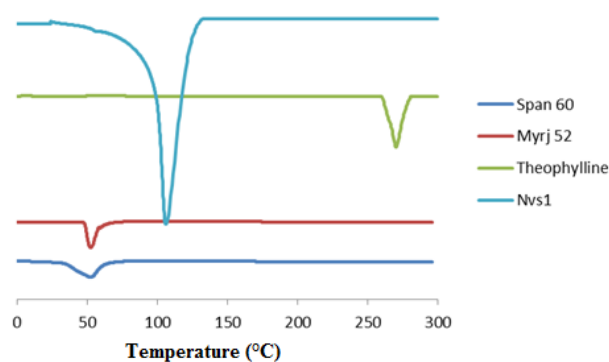


Figure 5: DSC thermogram of TN, Span 60, Myrj 52 and TN-loaded nanovesicles.

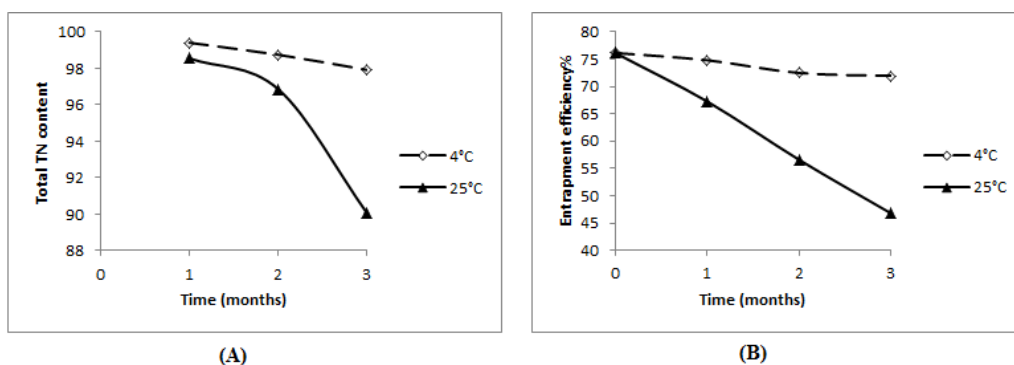


Figure 6: Effects of storage temperature on; total drug content (A) and entrapment efficiency (B).